ARTICLE

Journal of Materials Chemistry
www.rsc.org/materials

Towards an understanding of (bio)silicification: the role of amino acids and lysine oligomers in silicification

David Belton, Gary Paine, Siddharth V. Patwardhan and Carole C. Perry*

Division of Chemistry, Interdisciplinary Biomedical Research Centre, School of Science, The Nottingham Trent University, Clifton Lane, Nottingham, UK NG11 8NS. E-mail: Carole.Perry@ntu.ac.uk

Received 9th February 2004, Accepted 10th May 2004
First published as an Advance Article on the web 8th June 2004

In order to understand the role that proteins play in the generation of well regulated biosilica structures we need to understand the contribution of the components, singly and in combination. To this end we have performed a systematic study of the effect of amino acids and small peptide oligomers on silica formation from aqueous solution. Silicas produced from a potassium silicon catecholate salt at *ca.* pH 7 in the presence of the amino acids (Gly, Arg, Asn, Gln, Glx, Ser, Thr, Tyr, Pro, Ala, Lys) at a 2 Si : 1 amino acid molar ratio have shown that these amino acids affect the kinetics of small oligomer formation, the growth of aggregate structures and the morphology and surface properties of the silicas produced. The effects seen during the early stages of oligomer formation carry through to the properties of the particles and aggregates produced after extended periods of reaction. The behaviour of the amino acids relates to the pI and hydrophobicity of the individual amino acids. The presence of the nitrogen containing amino acids generates larger particles and the presence of amino acids containing hydroxyl and hydrophobic groups generates silicas with smaller particles than are produced for silicas produced in the absence of amino acids. An extensive study of the effect of the number of lysine and glycine units per peptide was also performed (for lysine, 1–5 and *ca.* 150 and for glycine, 1,4,5). Increasing the number of glycine units per additive molecule had little effect on the kinetics, aggregation, sample morphology, surface area and porosity of the silicas produced. A distinct relationship between the number of lysine units per additive molecule and an increased rate of oligomer formation, aggregate growth and a reduction in silica surface area and broadening of pore sizes was observed. A distinct change over in behaviour, particularly in regard to the porosity characteristics of the silica produced was noted for between $(lys)_3$ and $(lys)_4$ as well as this being the smallest size of peptide that was incorporated into the siliceous material formed. Aggregation was observed to accelerate exponentially over the full range of lysine oligomers used. Consecutive sequences of the same amino acid residues were shown to produce effects much larger than the sum of the effects of the individual residues, and at extremes mediate macroscopic morphological changes. The consequences of these findings for biosilicification are discussed. It is clear that all amino acid functional groups in proteins that are accessible to silica during the stages of formation from orthosilicic acid through to the final material have a role to play in determining the physical nature and structure of the material that forms.

Introduction

Scientists have been interested in biomineralisation for many years not only as a result of the sophistication that is achieved in the form of the crystalline and amorphous biomineral structures but also because composition and growth are so clearly regulated both spatially and temporally with minerals being produced under benign reaction conditions.[1] Furthermore, biominerals are extremely fine examples of organic–inorganic hybrid materials where the properties of the two phases when present together are more than the sum of their parts with peculiar strengths, resistance to degredation *etc.* being achieved.[2] These materials and new materials produced as a consequence of understanding the chemistry and biology used to form them could have tremendous technological implication in the development of materials and biomaterials with superior properties to those currently available.[3,4] Formation of ornate biosilica structures is of particular interest due to the peculiar physical and chemical nature of biosilica.[5–7] The silicas so formed show control of particles sizes, aggregation patterns and surface chemistry,[8–10] properties that are difficult to control during conventional syntheses. In addition, as the market for silicon-based materials is vast,[11] it is important to investigate the mechanisms underpinning the formation of biosilicas as an understanding of the processes may help us to develop novel silicon-based materials for potential application in areas as diverse as photonics, catalysis and biotechnology including drug delivery.[8] Biosilicas are formed in the presence of protein containing molecules with such molecules being isolated from the biogenic silica of higher plants,[12,13] sponges[14] and diatoms.[15–17] The proteinaceous materials have been proposed to regulate biosilicification *in vivo* in their respective systems.

In order to understand the role(s) of various biomolecules in biosilicification, various *in vivo* and *in vitro* studies have been undertaken. In particular, bioextracts from *Equisetum telmateia* and *Equisetum arvense* plants have been studied.[13,18] Upon amino acid analysis of the protein extracts, it was revealed that they contain relatively high amounts of proline and acidic residues (glutamic acid and aspartic acid) although it should be noted that the analysis procedure was not able to distinguish if the acids or their amide counterparts were originally present in the extracted proteins. When studied for their interaction with silicic acid, the bioextracts were found to direct the formation of silica in model studies performed *in vitro*.[8,13,18] These bioextracts when present at 1% by weight of the precipitatable silica (approximating to the living system), affected the kinetics of oligomer formation, reduced the primary particle size of silica from 4 nm to less than 2 nm and led to some crystalline silica being produced from aqueous solution at room temperature and pressure. Particular protein

DOI: 10.1039/b401882f

conformations and the interaction of protein with silicic acid at the molecular level were proposed as possible factors governing silica formation in the study. Sumper and co-workers have identified a set of biomolecules, which were later proposed to facilitate (bio)silica formation based on their activities *in vitro*. One diatom species—*Cylindrotheca fusiformis*—was principally used for investigations. It was found that ammonium fluoride treatment of silica cell walls released "native" silaffin proteins—natSil-1A (6.5 kDa), natSil-1B (10 kDa) and natSil-2 (40 kDa). Based on the *in vitro* studies, it was proposed that the combined activity of natSil-2 and natSil-1A or long-chain polyamines may control the formation of silica structured *in vivo*.[17,19] The marine sponge *Tethya aurantia* contains 75% dry weight silica in the form of needle like spicules that were used to isolate proteins that facilitate biosilicification.[14] It was found that each spicule contained a central filament of protein. After various treatments to dissolve the mineral silica from the sponge, three similar proteins were isolated and these silica proteins were named as silicatein α, β and γ. Silicatein α, which was found in the largest quantities, contained regular arrays of hydroxyls and was found to be highly similar to members of the cathepsin L and papain family of proteases. When exposed to a silica precursor, particulate silica formation was reported on the surfaces of the silicatein protein.[20]

It is worth nothing that the silaffin proteins, silicatein proteins and proteins extracted from grasses failed to produce structures that resemble the complex biosilica structures. Hence, in order to better understand the role(s) of various biomolecules in silicification, we present a systematic model silica synthesis study in the presence of various amino acids. Our initial interest was in investigating the role of glutamic acid/glutamine, aspartic acid/asparagine and lysine in silicification due to their high contents in the bioextracts obtained from grasses.[12,13,18] Other amino acids, representative of the main groups of functionality have also been chosen for study. Although the effect of some amino acids and oligomers on specific aspects of silica formation have been previously reported, it is noted that they were used when the hydrolysis of tetraethoxysilane (TEOS) was studied.[21] In that study, it was reported that tetralysine and polylysine were both able to enhance the hydrolysis of TEOS. Polyamino acids including polylysines of varying extended chain lengths have also been found to affect silicification.[22,23] The polyamino acids were proposed to bring silicic acids monomers and oligomers closer to each other by electrostatic attractions, which in turn may favour condensation to produce silica.[22]

In the current study, it is also our aim to determine the effect of the size of small lysine oligomers (keeping the overall concentration of functional groups constant) on the different stages of silicification. We want to identify the minimum chain length of lysine oligomers required to show significant effects on silicification kinetics, particle aggregation, particle growth and/or final product properties. A comparison was made with the effect of small oligomers of glycine on silicification.

Various silica precursors have been used in model studies of silicification. In particular, the use of tetramethoxysilane,[17,24] tetraethoxysilane,[21,25] sodium silicate (water glass),[26] silica sol,[22] tetrasodium monosilicate *n*-hydrate[27] and various silicon catecholate salts—$M_2[Si(C_6H_4O_2)_3]\cdot xH_2O$ (M = Li, Na, K, NH_4 and NEt_3H)[28] have been reported in the literature. The precursor used in this investigation was the water soluble potassium catecholato-complex of silicon that can be hydrolysed upon neutralising to pH 7 to release orthosilicic acid.

Experimental

Reagents

Dipotassium silicon triscatecholate ($K_2[Si(C_6H_4O_2)_3]\cdot 2H_2O$ (97%)), L-amino acids, L-lysine oligomers (99%), L-glycine oligomers (99%), poly L-lysine (97%, mw 15000–30000) and anhydrous sodium sulfite (97%) were purchased from Sigma Aldrich Chemicals; ammonium molybdate·$4H_2O$, hydrochloric acid (37%) and sulfuric acid (98%) were purchased from Fisher Scientific; oxalic acid·$2H_2O$ (99%) and *p*-methylamino phenol sulfate (99%) were purchased from Acros Chemicals and standard stabilised silicate solution (1000 ppm as SiO_2) was purchased from BDH. All chemicals were used without further treatment. Distilled deionised water (ddH_2O) having a conductivity less than <1 $\mu S\ cm^{-1}$ was used. The purity of the potassium tris(catecholato)silicate(IV) complex was checked by ^1H NMR (single peak at 6.63 ppm for complexed protons).

Silica synthesis and kinetic studies

Experiments to study the oligomerisation reactions were carried out at room temperature (293 $\pm$ 2) K. Solutions (30 mmol l^{-1}) were made up with doubly distilled water in plastic containers. The amino acid additives, when required were added immediately prior to acidification and the pH of the resulting solutions was lowered to 6.8 $\pm$ 0.20 by addition of a known amount of 2 M hydrochloric acid and the pH monitored for the duration of the experiment. Experiments using the lysine oligomers were performed as above except that the solution containing the lysine oligomers had its pH altered prior to mixing with the silicon complex to ensure that any interactions that occurred were with functional groups in the form present at pH 7.0. The subsequent decomposition of the complex to orthosilicic acid and oligomerisation of the newly formed silicic acid was measured as a function of orthosilicic acid concentration by a modification of the molybdenum blue colorimetric method described by Iler.[29] 10 microlitre aliquots of solution were removed and added to solutions containing 15 ml of distilled water and 1.5 ml of an acidic solution containing ammonium molydate and the resulting solution allowed to stand for 15 min, thereby allowing any dimers present to decompose to monomers which could be detected by the colorimetric method. 8 ml of a reducing solution containing Metol was then added and the absorbance of the blue silicomolybdate complex measured after 2 hours at 810 nm using a Unicam UV2 UV-VIS spectrometer. Calibration of this method using a standard silicate solution [BDH] showed a linear relationship between concentration and absorbance over the whole of the concentration range used (0–35 mmol dm^{-3}) and an experimental error in measurement of $\pm$1.0%. Orthosilicic acid concentrations were measured at intervals between 0.5 and 240 min after the initial pH reduction with 20–30 measurements being taken within the first hour. The equilibrium orthosilicic acid concentration (for an individual system) was reached within 2 hours reaction. Readings were continued for the first 24 hours of reaction with the precipitated silica being removed after 168 hours of reaction, washed three times with distilled water to remove traces of catechol and other solution species, centrifuged at 8000 rpm, rapidly frozen in liquid nitrogen and freeze-dried at 223 K using a Christ alpha 1–4 freeze-dryer.

Residual complex concentrations were determined by solution ^1H NMR spectroscopy at selected time points during reaction. Measurement of the peak area arising from the complex (a single peak at 6.63 ppm downfield from sodium-3-trimethylsilyl propionate-2,2,3,3-d_4 (TSP)) and comparison to the peak area for signals arising from the ligand alone in relation to known amounts of TSP enabled calculation of complex concentrations during the silicification reaction. After initiation of the reaction, solution complex concentrations immediately reduced to 0.1–0.7 mmol l^{-1} meaning that the majority of the silicon species were available for oligomerisation and for production of silica. Solution data were manipulated according to Harrison and Loton[28] and time periods when the dominant molecular reaction followed third order

kinetics (the formation of trimers from monomers and dimers), reversible first order kinetics (the addition or removal of orthosilicic acid to/from trimers or larger oligomers) or Ostwald ripening was the dominant reaction (with little measurable change in the concentration of silicic acid being detected) were obtained. For the period where apparent third order kinetics were followed, a plot of $1/[Si(OH)_4]^2$ *vs.* time gave a straight line with the rate constant being obtained from the gradient of the plot. For the period where reversible first order kinetics were followed a plot of $\ln(A - A_t)$ *vs.* time gave a straight line of slope $(k_+ + k_-)$ where A is the concentration at any time and A_t the concentration of orthosilicic acid at equilibrium (here taken as the value measured after 24 hours reaction). The separate rate constants for the forward and reverse reaction were obtained using the equilibrium constant K, which is the ratio of the forward and reverse rate constants and is also the ratio of the oligomerised silica and the equilibrium concentration of orthosilicic acid present in solution.[28]

Photon correlation spectroscopy

Samples were also prepared for dynamic light scattering analysis. Samples were taken from the orthosilicic acid condensation experiments immediately on pH adjustment (amino acid study), or mixing (lysine oligomer study), and filtered through a 200 nm membrane into a 1 cm polymethylmethacrylate cell. Aggregation of silica particles was then monitored over a 40 hour period using a Coulter N4 plus photon correlation spectrometer with a He–Ne (632.8 nm) laser supply. All measurements were carried out at an angle of 90° and at 293 K. Measurements obtained were averages of the data collected over intervals of 2 to 60 minutes, the time selected depending on the rate of particle growth. Values of particle size are presented for comparative purposes and should not be taken as absolute values and are here referred to as 'apparent' particle size.

Scanning electron microscopy

For SEM studies, lyophilised samples were dispersed onto double-sided sticky tape and mounted on aluminium stubs with the edges of the sticky tape being painted with quick drying silver paint to prevent charging of the sample. All loose aggregates were removed by tapping the stub before the silica samples were gold coated with an argon plasma at 1.2 kV and 4 mbar pressure for 2 minutes using an Edwards S150B sputter coater. Images were acquired using a JEOL JSM-840A scanning electron microscope with an accelerating voltage of 20 kV. Average particle sizes were calculated by measuring all distinct particles within 1 μm^2 areas and averaging. If this proved impossible particle sizes were measured over larger areas of the obtained images.

Surface area analysis

Surface area measurements were obtained from 12–30 mg quantities of precipitated silica obtained after 168 hours reaction. Single point measurements and full BET isotherms were obtained using a fully automated Micromeritics Tristar 3000 (Ineos Silicas, Warrington). Samples were degassed at 403 K for a minimum of 16 hours before analysis at liquid nitrogen temperatures. The specific surface area was obtained *via* the BET method[30] where nitrogen is assumed to have a cross-sectional area of 0.16 nm^2. Pore size distributions were calculated by the application of BJH theory[31] to the desorption branch of the isotherms as all samples showed similar adsorption/desorption behaviour.

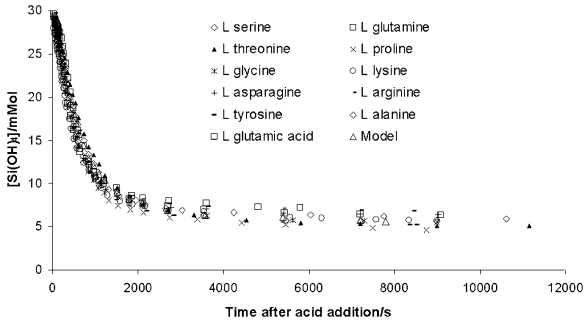

Fig. 1 Changes in orthosilicic acid concentration with time following initiation of the reaction by pH reduction to 7.0 for a 30 mmol dm^{-3} solution of $K_2[Si(Cat)_3]\cdot 2H_2O$ in the presence of 15 mmol dm^{-3} of selected amino acids.

Thermal gravimetric analysis

The organic material associated with the sedimentable silica was detected by thermal gravimetric analysis. Analysis was performed under nitrogen using a Stanton Redcroft TG 760 furnace, balance controller and UTP temperature controller with a heating rate of 10 K min^{-1} with data being sampled every 30 seconds. Entrained organic content was calculated by comparison of weight loss between 400 and 800 K relative to the silica produced from the catecholate complex alone.

Results

Solution chemistry

The residual undissociated complex for reactions performed in the presence of a 1 amino acid : 2 silicic acid molar ratio after 24 hours reaction varied from 0.2–0.6 mmol dm^{-3}, corresponding to an initial orthosilicic acid concentration for the condensation experiments of 29.4 to 29.8 mol dm^{-3} (98–99%). The pH of all solutions was in the range 6.8 $\pm$ 0.2. Silicic acid concentrations were monitored from 30 seconds after initiation of the reaction (by lowering of pH or mixing) until 24 hours of reaction had elapsed, Fig. 1 shows plots of silicic acid concentration with time in the presence of amino acids. The data for the blank model sample is shown for comparison. Table 1 lists the third order and apparent first order rate constants for the reactions performed in the presence of the amino acids. None of the experiments showed a dominant dimerisation phase where no loss in silicic acid with time was observed.

The region of 3rd order dominance occurred during the first 3 minutes of condensation for reaction with all the amino acids studied. Increased rates of condensation were observed for arginine, asparagine, lysine and glutamine and slower rates of condensation, compared to the blank system for reactions

Table 1 3rd and 1st order rate constants for orthosilicic acid condensation in the presence of selected amino acids

Amino acid	3rd k/ 10^{-6} mM^{-2} dm^6 s^{-1}	1st order condensation rate constant k_+/s^{-1}	1st order dissolution rate constant k_-/s^{-1}
Ser	0.97	0.001362	0.000238
Gln	1.56	0.001425	0.000275
Thr	0.48	0.001062	0.000138
Pro	1.18	0.001237	0.000163
Gly	0.84	0.001452	0.000248
Lys	1.62	0.001451	0.000249
Asn	1.60	0.001446	0.000254
Arg	2.04	0.001163	0.000237
Tyr	1.30	0.001318	0.000183
Ala	0.89	0.001225	0.000175
Glu	0.605	0.00129	0.00021
Blank	1.30	0.001201	0.000199

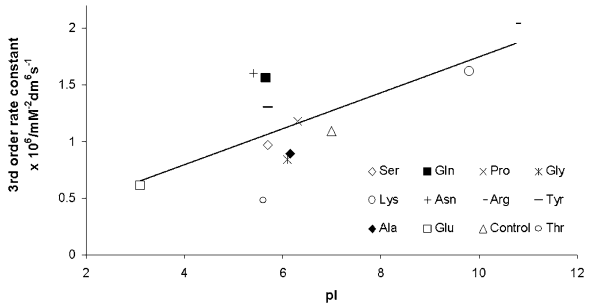

Fig. 2 The relationship between the 3rd order rate constant for the formation of trimers from monomer and dimer of orthosilicic acid and isoelectric point of selected amino acids. The line shows the trend only.

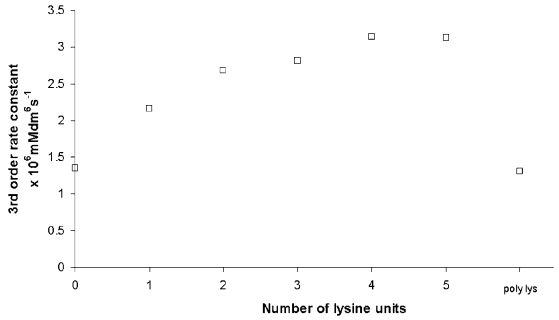

Fig. 3 The effect of the number of lysine units per molecule on the 3rd order rate constant for the formation of trimers from a monomer and dimer of orthosilicic acid.

performed in the presence of threonine and glutamic acid (Fig. 2). The reversible 1st order region dominated from about 4 to 12 minutes in each of the experiments but with less influence of the amino acids when compared with the 3rd order region. By the end of the reversible 1st order region (after $\sim$12 minutes) between 50 and 60% of the available orthosilicic acid had condensed to trimers or larger oligomers. All of the systems showed a continued reduction in orthosilicic acid over the 24 hour period investigated with a range of rates between 1.2–2.1 $\times$ 10^{-3} mmol dm^{-3} min^{-1}. Final orthosilicic acid concentrations ranged from 3.5 to 5.0 mmol dm^{-3}. At the end of the 24 hour period all but proline had formed a clear weak gel which could be broken by very gentle agitation. In the case of experiments performed in the presence of proline a grainy sediment was formed as observed by the naked eye.

For reactions performed in the presence of L-lysine homopeptides the residual undissociated complex varied from 0.1 to 0.7 mmol dm^{-3}, corresponding to an initial orthosilicic acid concentration of 29.3 to 29.9 mmol dm^{-3} (98–99%). The pH of the solutions prepared using the shorter peptides was 6.8 $\pm$ 0.2, but that of reactions performed in the presence of poly L-lysine was 6.4. On addition of polylysine to the complex an immediate precipitate was formed. This was not thought to be silica as a molybdenum blue assay of the homogenised mix still gave an orthosilicic acid concentration of *ca.* 30 mmol dm^{-3}. It is suggested that the precipitate may have been the complex cationically exchanged with polylysine amine side chains in place of potassium. Separation of the precipitate from the supernatant immediately after mixing resulted in a reduction of orthosilicic acid being detected commensurate with about 20% of the available silicon being associated with the polylysine. This factor was presumably responsible for the reduced condensation rates and a lower pH being observed during the early stages of reaction. If the precipitate was allowed to remain in the reaction mixture it was observed to slowly re-dissolve during the course of the experiment and the orthosilicic acid concentration measured at the end of the experiment was found to be in line with all other experiments.

Table 2 lists the apparent third order and first order rate constants for the reactions performed in the presence of the lysine homopeptide. The 3rd order rate constant was observed to increase with increasing lysine oligomer chain length from 2.2 $\times$ 10^{-6} mmol^2 dm^{-6} s^{-1} for the monomer to 3.2 $\times$ 10^{-6} mmol^2 dm^{-6} s^{-1} for the tetramer and pentamer. This compares with a value of 1.3 $\times$ 10^{-6} mmol^2 dm^{-6} s^{-1} for reactions conducted in the absence of lysine and its oligomers, Fig. 3. Increasing glycine oligomer length, on the other hand, showed little effect on the 3rd order rate constant (0.8 $\times$ 10^{-6}–1.0 $\times$ 10^{-6} mmol^2 dm^{-6} s^{-1}; data not shown). The onset of the 3rd order region appeared to be slightly delayed with increasing oligomer chain length, data not presented.

The effect of the additives on the reversible 1st order region was less well defined, but suggested a slight increase in the rate of the forward reaction with increased oligomer length. First order kinetics dominated from around 5 to 12 minutes in all systems, during which time the available orthosilicic acid concentration fell to around 40% for the short oligomers. Over the course of 24 hours of reaction the concentration of orthosilicic acid fell to between 4.0 and 6.7 mmol dm^{-3} which were values in excess of those monitored for the blank system. At the end of the 24 hour period the samples were homogenous but had become increasingly cloudy with increasing homopolymer length but with no visible sedimentation although a sediment could be formed on gentle agitation of the solutions.

Table 2 3rd and 1st order rate constants for orthosilicic acid condensation in the presence of L-lysine homopeptides

Homopeptide	3rd order rate constant $k/10^{-6}$ mmol^2 dm^{-6} s^{-1}	1st order condensation rate constant k_+/s^{-1}	1st order dissolution rate constant k_-/s^{-1}
lank	1.30	0.0013	0.0002
Lys	2.16	0.0014	0.0002
$(Lys)_2$	2.68	0.0014	0.0004
$(Lys)_3$	2.81	0.0014	0.0003
$Lys)_4$	3.14	0.0014	0.0003
$(Lys)_5$	3.13	0.0016	0.0003
$(Lys)_{poly}$	1.31	0.0009	0.0003

Photon correlation spectroscopy

Data obtained by photon correlation spectroscopy are presented in Fig. 4 and 6 for experiments conducted in the presence of amino acids and oligomers of lysine respectively. Rates of aggregation are compared by analysis of the maximum growth rates in terms of volume increase of apparent particle size with time, Fig. 5 and 7. For experiments conducted in the presence of amino acids, maximum aggregation rates were observed for L-arginine and L-lysine (5.0 and 3.3 nm^3 min^{-1} respectively) compared to a value of 1.4 nm^3 min^{-1} for reactions performed using the catecholate complex alone. The lowest rate was observed for L-glutamic acid of 1.3 nm^3 min^{-1}.

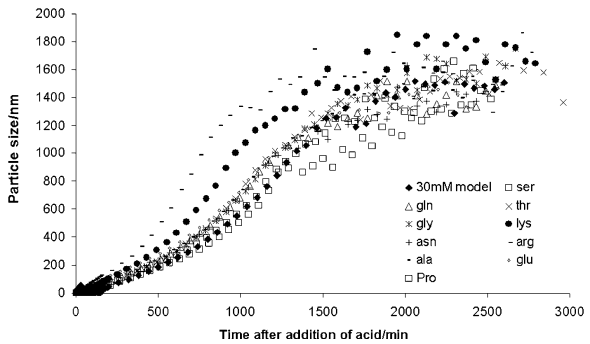

Fig. 4 Photon correlation spectrometry of silica aggregating in the presence of selected amino acids.

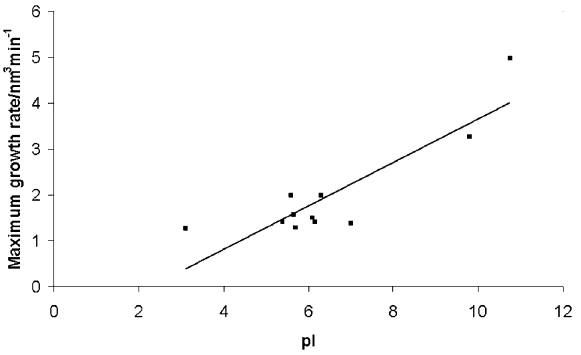

Fig. 5 Maximum growth rate of the structures as measured by photon correlation spectroscopy in relation to the isoelectric points of the side chain functional groups of selected amino acids. The line shows the trend only.

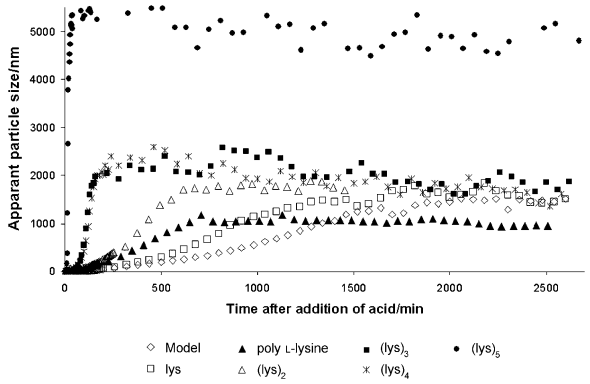

Fig. 6 Photo correlation spectra obtained from 30 mmol l^{-1} solutions of $K_2[Si(Cat)_3]\cdot 2H_2O$ in the presence of $(lys)_n$ where the total concentration of the lysine functional groups is 15 mmol l^{-1} over a period of 40 hours reaction.

For all systems a growth boundary was observed where there was an increased scatter in the data which was also marked by a decrease or cessation in the aggregation growth. The shortest times for this boundary were observed for L-arginine and L-lysine (1000 and 1300 min respectively), for all others the time was between 1500 and 1600 min. The rates and boundary times were found to be largely in line with the pI of the amino acids and was shown to be most significant where the amino acid side chains were expected to be charged at the pH of the experiments, Fig. 5.

For precipitation experiments performed in the presence of L-lysine homopeptides, aggregation rates were dramatically increased with lysine units from 3.3 nm^3 min^{-1} to 103 $\times$ 10^6 nm^3 min^{-1} for the range mono to penta L-lysine, Fig. 6, 7. Apparent maximum particle size increased from mono to penta L-lysine from 1800 nm to 5900 nm, Fig. 7. The boundary times decreased with increased L-lysine number from 1640–40 minutes and were followed by a period of contraction observed for di

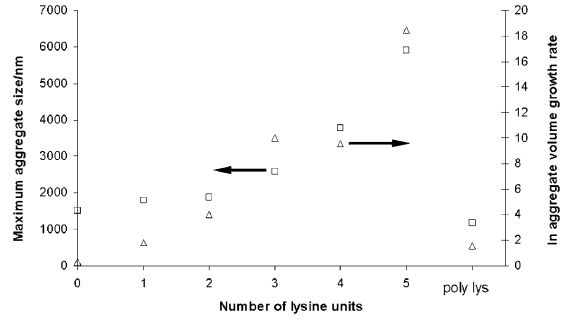

Fig. 7 Maximum growth rate and maximum apparent particle size for silica aggregating in the presence of lysine oligomers.

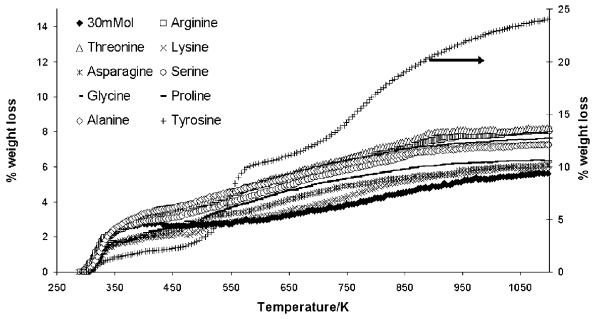

Fig. 8 Thermogravimetric analysis of silicas condensed in the presence of selected amino acids.

L-lysine to penta L-lysine but not for reactions carried out in the presence of the monomer or for the control reaction. Glycine oligomers showed little change in the aggregation rate (1.5–2.6 nm^3 min^{-1}), boundary times were all $\sim$1500 min and no subsequent contraction was observed (data not presented).

Residual organic material in sedimented silica

Residual organic material entrained within the sedimentable silica (not removed on washing with distilled water) was determined as the weight lost during thermogravimetric analysis over the temperature range 400–800 K after subtraction of the underlying loss of weight through silanol condensation over the same range (*i.e.* for the blank system), Fig. 8 and 9. This temperature range corresponded to the thermal decomposition of organic compounds and resulted in the loss of CO_2, H_2O, NH_3 and some short chain volatile rearrangement products. In the experiments carried out under nitrogen, darkening of samples was observed, which may indicate the possibility of the presence of residual organic matter.

For silicas condensed in the presence of amino acids, only materials prepared in the presence of L-tyrosine showed a significant weight loss over the temperature region highlighted. This was thought to be due to its low water solubility rather than its incorporation into the silica matrix.

The L-lysine homopeptides showed increasing incorporation with increasing chain length with 9% penta L-lysine retained and 18% poly L-lysine retention, Fig. 10. Glycine oligomers by comparison showed little organic componant in the silica produced—the maximum found was $\sim$0.5% in pentaglycine (data not presented).

Gas adsorption analysis

Silica samples produced in the presence of amino acids gave type IV isotherms with H2 hysteresis typical of micro/mesoporous materials. Surface area analysis by the BET method gave values between 538 and 730 m^2 g^{-1}. A correlation between surface area and side chain hydrophobicity was

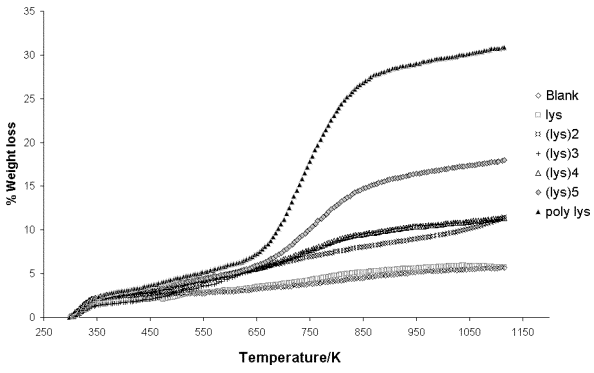

Fig. 9 Thermogravimetric analysis of silicas produced in the presence of $(lys)_n$.

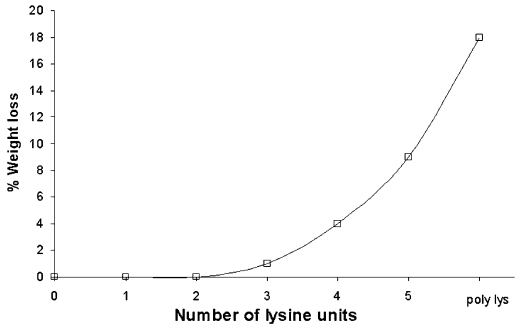

Fig. 10 Relationship between % organic material retained in silica with number of lysine units in homopeptide.

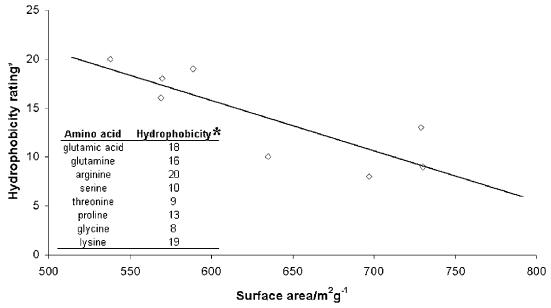

Fig. 11 Relationship between surface area and order of hydrophobicity[32] of selected amino acids for silica condensed in their presence. The line shows the trend only.

observed, Fig. 11, the most hydrophobic amino acids producing the largest surface areas. The order of hydrophobicity was based on physicochemical properties of amino acid side chains.[32] Values of hydrophobicity were arbitrarily assigned as 1–20 for the most hydrophobic to the least hydrophobic functional side chain.

Adsorption/desorption isotherms for the silicas prepared in the presence of the small (1–3) lysine oligomers gave type IV isotherms with H2 type hysteresis typical of micro/mesoporous materials. For silicas prepared in the presence of the larger peptides the hysteresis was observed to shift to higher partial pressures. A decrease in surface area was observed with increasing chain length, Fig. 12. Little change in pore volume and increases in average pore diameter were also observed. There was a general trend towards reduced micropore volumes and increasingly disperse and enlarged mesopores with increasing lysine peptide chain length, Fig. 13. The material changed from predominantly mesoporous to predominantly macroporous as the peptide length increased from 3 to 5, Fig. 14. For silica prepared in the presence of polylysine a range of both mesoporous and macroporous pores was observed, perhaps due to silica being deposited at different time periods in the silica precipitation reaction due to the initial presence of the polylysine–silicon complex aggregate that was observed to form.

Scanning electron microscopy

In the case of silica formation without any additive, the typical average particle size as observed by SEM was 77 nm as shown

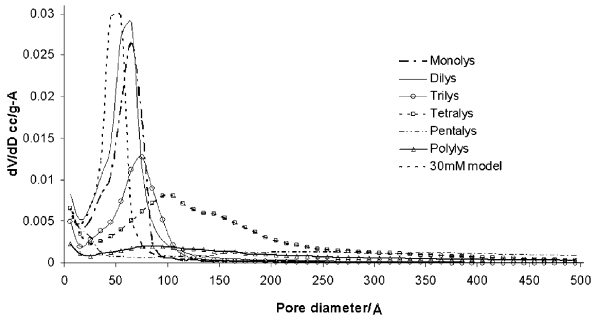

Fig. 13 Pore size distributions for silicas produced in the presence of $(lys)_n$.

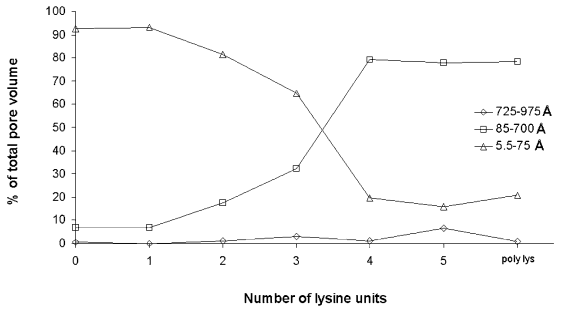

Fig. 14 Relative pore volumes of different size domains of pores in silicas produced in the presence of $(lys)_n$.

in micrograph H in Fig. 15. In the presence of the nitrogen containing amino acids considered here, larger particles were observed. In particular, the average particle size in the case of arginine (micrograph A, Fig. 15) was 123 nm and that for asparagine (micrograph B, Fig. 15) was 175 nm. All silicas synthesised in the presence of nitrogen-containing amino acids produced materials with granular appearance. Silica prepared using lysine and glutamine (micrographs G and E respectively in Fig. 15) contained particles of average size of 108 and 140 nm respectively. Furthermore, addition of lysine and glutamine to the reaction medium were also found to alter the macroscopic morphology of the silica. As shown in the inserts of micrographs E and G in Fig. 15, it can be seen that both amino acids produced silica with sharp edges, while no such morphologies were observed in the other samples. The presence of proline in the reaction medium produced a granular silica with average particle size of 114 nm, micrograph A of Fig. 16.

Hydroxyl containing amino acids decreased the granular appearance of the silica produced. Serine, threonine and tyrosine were found to produce silica with "smooth" surface morphology as respectively shown in micrographs B, C and D in Fig. 16. These amino acids affected the macroscopic nature of silica to a limited extent.

Finally, glycine and alanine had little effect on the silica produced in their presence. The average particle sizes of silica synthesized in the presence of glycine and alanine were 84 and 48 nm respectively and more open flaky structures were formed. Although glutamic acid did not affect the particle formation on the microscopic scale, various large aggregates were observed (see micrograph C in Fig. 15).

Based on the data presented herein on the role of amino acids

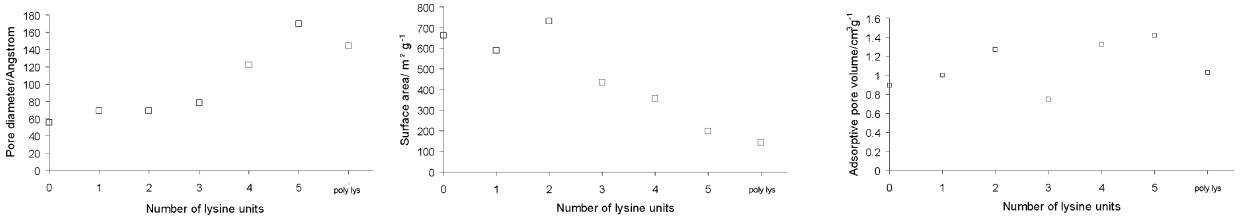

Fig. 12 Surface area, pore volume and average pore diameters for silicas produced in the presence of $(lys)_n$.

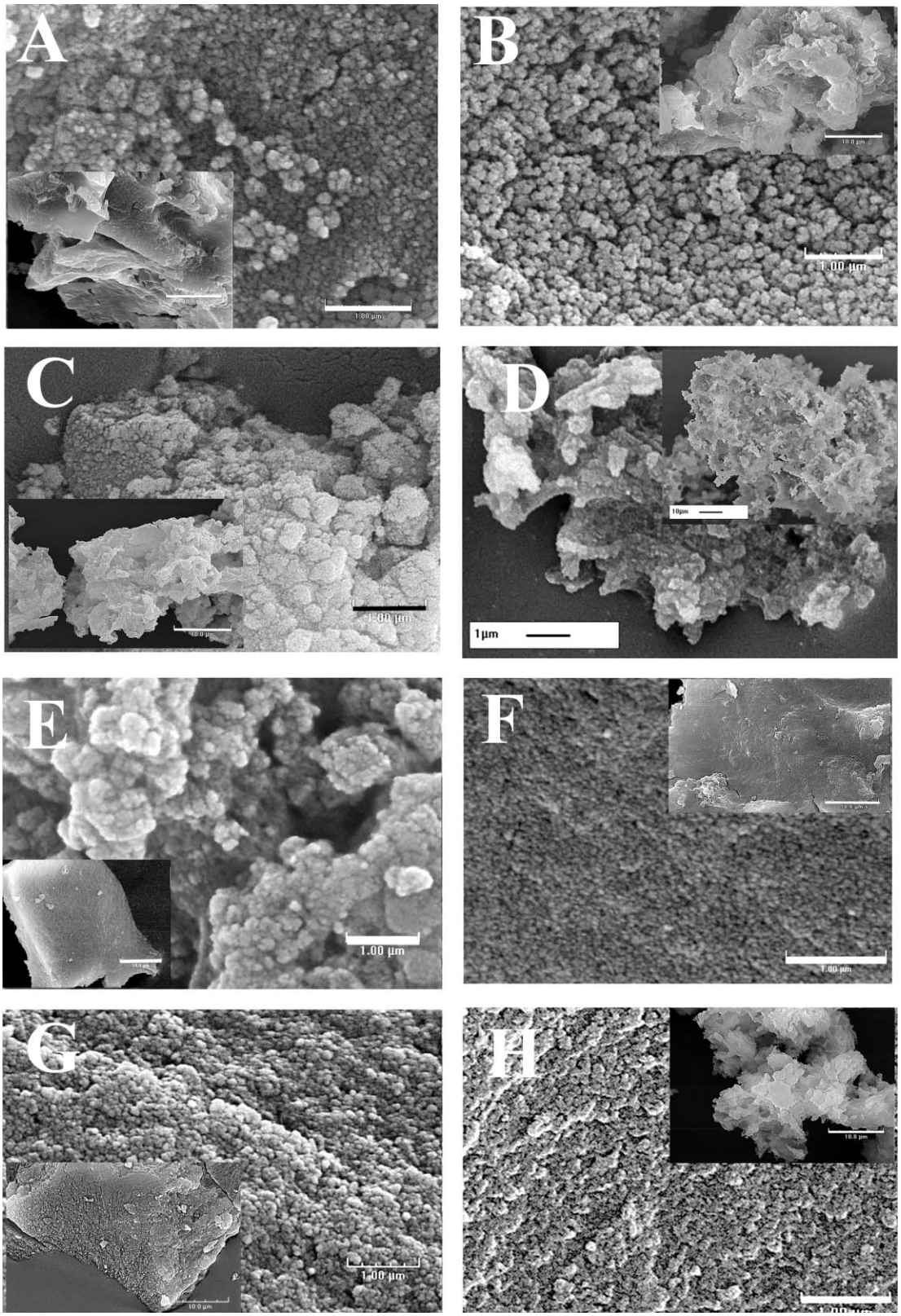

Fig. 15 Scanning electron micrographs of silicas produced in the presence of selected amino acids. A. arginine, B. asparagine, C. glutamic acid, D. glycine, E. glutamine, F. alanine, G. lysine, H. blank. Scale bars represent 1 μm (inserts 10 μm).

in silica formation, it is clear that all the nitrogen-containing amino acids investigated have an effect on the aggregation of silica particles. In order to investigate this phenomenon in detail and to explore the mechanism of the interaction, we further studied the effect of one specific amino acid (lysine) and its oligomers on silicification. Silica formation was carried out in the presence of di-, tri-, tetra-, penta- and poly-lysine samples. The representative SEM data of silica synthesized in the presence of lysine oligomers are presented in Fig. 17. The formation of distinct silica particles/aggregates was observed in the presence of lysine oligomers. The average particle sizes of silica particles formed using di-lysine, tri-lysine, tetra-lysine, penta-lysine and poly-lysine where the concentration of side chain functionalities was kept constant were respectively 108, 139, 85, 109, 122 and 467 nm. Comparatively larger particles were formed when poly-lysine was used as an additive. It

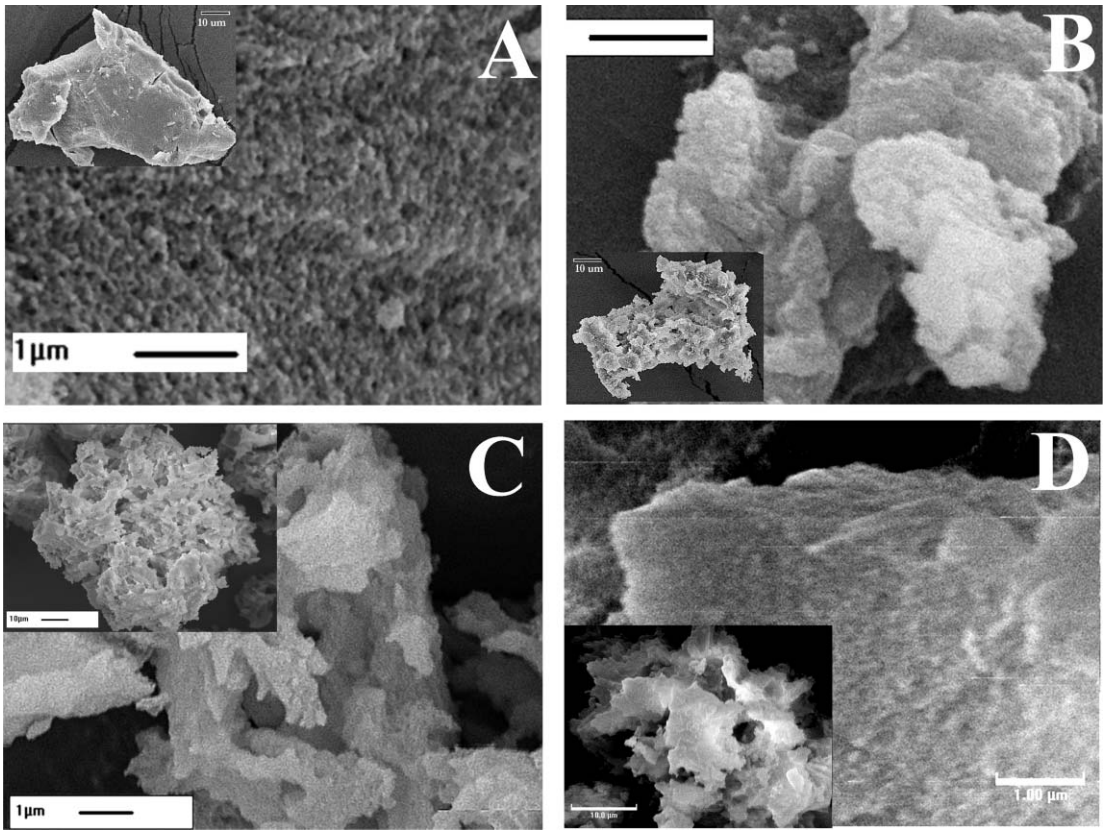

Fig. 16 Scanning electron micrographs of silicas produced in the presence of selected amino acids. A. proline, B. serine, C. threonine, D. tyrosine. Scale bar represents 1 µm (inserts 10 µm).

should be noted that silica particles of similar sizes have been previously synthesized in the presence of poly-L-lysine using various other silica precursors such as tetramethoxysilane, ethylene glycol modified silane and water glass.[33,34] In our previous experiments on silica precipitation using bioextracts isolated from horsetail ferns, it was found that these bioextracts were able to direct the formation of crystalline domains within the siliceous material.[13,18] In order to assess any similar structure direction in the current investigation, X-ray diffraction and selected area electron diffraction studies were performed. In the investigated samples, there was no evidence for the presence of any crystallinity (data not presented).

Discussion

Solutions of orthosilicic acid at a concentration of 30 mmol dm^{-3} were rapidly formed at circumneutral pH by the acid dissociation (>98% complete) of the complex $K_2[Si(C_6H_4O_2)]\cdot 2H_2O$. This allowed the early stages of condensation of orthosilicic acid in an aqueous environment to be followed in the absence of interference from continued hydrolysis of organosilicon species. This is in direct contrast to model studies using organosilane precursors such as tetramethoxysilane where a complex mixture of oligomers (some alkoxylation is still present) is generated within 15 minutes of its hydrolysis with only 20% of the initial silicic acid available (data not included) for reaction with any additives that are introduced at this point into the reaction environment.[17,19,35]

The initial dimerisation stage of the process is not detected by the molybdenum blue method since the dimer dissociates within the time of the silicomolybdic acid complex development so no apparent loss of orthosilicic acid is detected. This has sometimes been referred to as the induction period. During the next (3rd order) stage monomers and dimers condense so that the apparent reduction in orthosilicic acid concentration is the combined effect of monomer and dimer loss. Beyond this region, since monomer condensation on to existing oligomers occurs in preference to oligomer co-condensation, reversible 1st order kinetics are observed as a competing dissolution of monomer back in to solution occurs.

The rate constant measured for the trimerisation stage was increased by the addition of nitrogen containing amino acids, particularly L-arginine and L-lysine, and was reduced for reactions performed in the presence of L-glutamic acid. This effect highlights the dependence of the early stages of condensation on the presence of anionic species since rates at neutral pH are controlled by relatively small populations of them; *e.g.*:

$$Si(OH)_3OSi(OH)_2O^- + Si(OH)_4 \rightarrow Si(OH)_3OSi(OH)_2OSi(OH)_2O^- + H_2O$$

Enhancement of anion formation in the presence of L-arginine and L-lysine, and suppression in the presence of L-glutamic acid would be expected and it appears to be the case. In addition to L-lysine and L-arginine, L-asparagine and L-glutamine were also able to affect the kinetics in the early stages of silicic acid condenstation. The role of these uncharged nitrogen side chains in accelerated condensation remains unclear.

The importance of positively charged nitrogen functional groups in regulating amorphous silica production was reinforced when increasing chain lengths of L-lysine homopeptides were used. Changes to the onset and cessation of the trimer stage were delayed slightly. The delay in the onset of the time period when third order kinetics dominated, assuming complex dissociation and dimerisation were unaffected would result in a higher population of the dimer at the onset of 3rd order kinetics and therefore higher rates of condensation if the process is largely dependent on the presence of anionic dimers. In studies of condensation of silicic acid prepared from sodium silicate solutions, a dramatic increase in condensation rates in

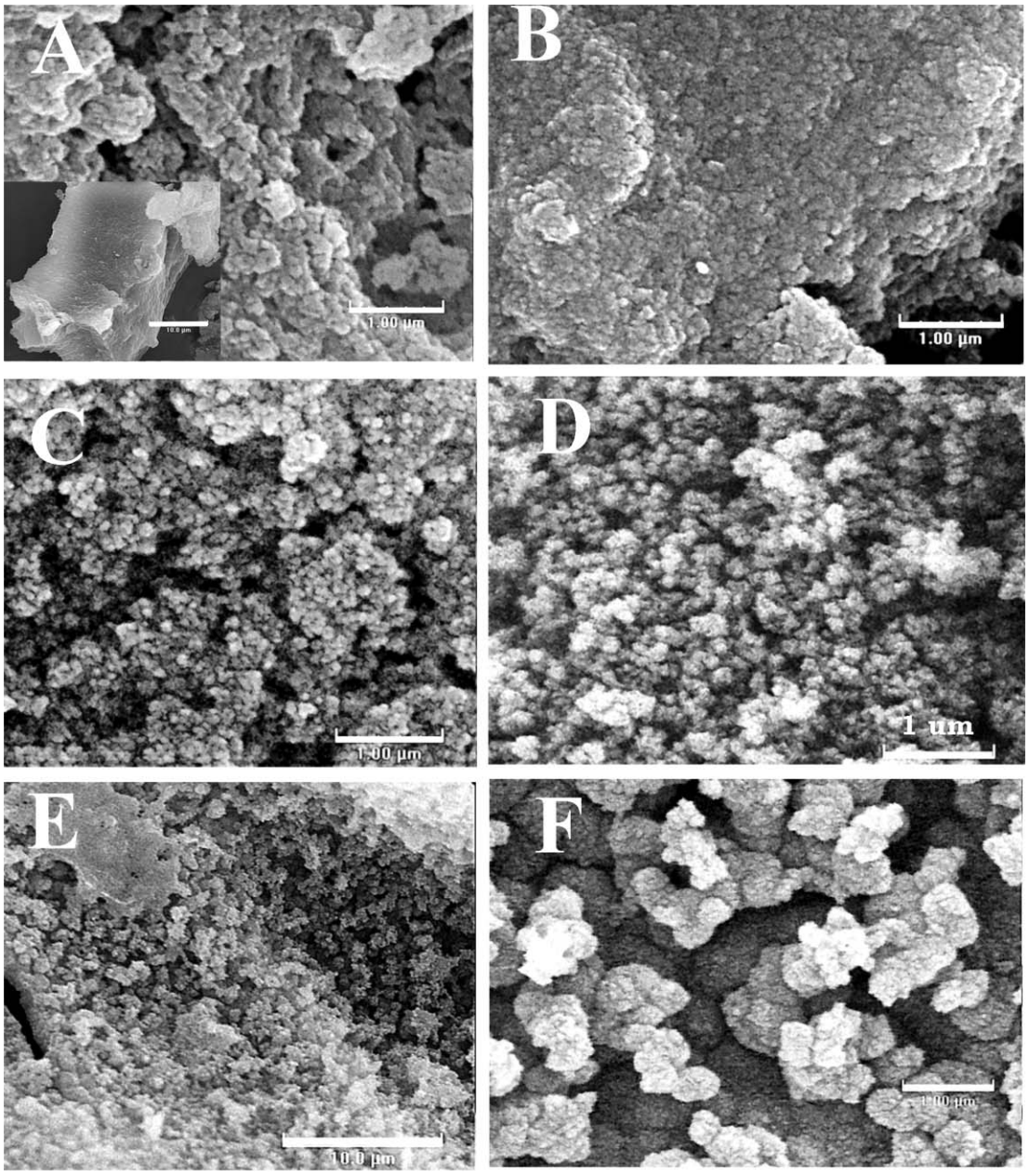

Fig. 17 Scanning electron micrographs of silicas produced in the presence of $(lys)_n$. A. $(lys)_2$, B. $(lys)_3$, C. $(lys)_4$, D. $(lys)_5$, E.and F. poly-lysine. Scale bars represent 1 µm for A–D, F and 10 µm for insert in A, E.

the presence of lysine and arginine homopeptides was reported.[22] These solutions were allowed to condense for 10 minutes prior to introduction of the peptides so would be expected to contain a significant population of silica oligomers. In this study amino acids and lysine homopeptides were added to a rapidly dissociating complex providing supersaturated monomeric silicic acid. The condensation rates in the early stages were found to be enhanced only moderately by comparison (approximate doubling of the 3rd order rate constant observed with $(lys)_5$). Co-addition of poly lysine and acid to the complex resulted in no observed immediate loss of molybdate active species, any precipitate formed was attributed to the formation of a cation exchanged poly lysine silicon catecholate complex with lower solubility than the potassium analogue. The indication was therefore that immediate silica precipitation previously reported was due to oligomer aggregation.[22]

Aggregation rates of the condensing silica observed by photon correlation spectroscopy showed increases for L-arginine and L-lysine. Although below neutral pH silica particles become less charged and tend to aggregate there is nonetheless a noticeable effect suggesting that residual surface charges are neutralised by the presence of the basic amino acid side chains. This effect was much more prominent for the aggregation of silica in the presence of the L-lysine homopeptides and suggests that these can cause bridging between particles similar to that described previously (refs. 22, 29 p. 386, 33*a*). The importance of the basic side chain on these homopeptides was demonstrated by the failure of L-glycine homopeptides to produce any effect. The increased apparent particle size observed with increased peptide chain length suggests that this bridging effect is strong enough to produce extended structures in solution but that they are too weak to survive the isolation process demonstrated by the absence of similar large scale structural changes observed by SEM.

The 'boundaries' observed in the PCS data are thought to occur at the stage where a continuous network of silica aggregates forms throughout the sample. The size fluctuations observed beyond this point are, we believe, due to structural inhomogeneities within this network. The subsequent general decrease in aggregate size in the systems involving lysine homopeptides could be a consequence of the bridging effect resulting in continued inter-particle silanol

condensation brought about by the more proximate neighbouring aggregates.

Removal of organic material by washing was achieved with all of the amino acid condensed silicas with the exception of L-tyrosine due to its relative insolubility in water. However increasing amounts of organic material were found in the lysine homopetide condensed silica with increased peptide chain length. That this is due in part to entrainment of the homopeptides in the pores formed as the silica particles condense together is in no doubt, but the failure of the glycine oligomers to be retained in the material to the same degree suggests a more involved role for the L-lysines, possibly in the formation of more inter-particle condensation brought about by extended contact times between the reacting species resulting in partial pore closure.

Changes in surface areas, pore volumes and average pore diameters obtained for silicas prepared in the presence of the L-lysine homopolymers are also indicative of a change in the structure of the siliceous materials produced as the oligomer chain length increased. A reduction in the surface area with increasing chain length occurs whilst at the same time the volume contribution from small pores also decreases, Fig. 14. The silicas change from being predominantly mesoporous to largely macroporous as the additives increase in length from tri L-lysine to penta L-lysine. Again this could be due to blocking of smaller pores by organic residues or through closure of pores through increased inter-particle condensation. It is also possible that some contribution to the measured porosity of the samples arises from pores present within aggregates.

The surface areas of the amino acid condensed silicas could in general be related to the hydrophobicity of the amino acid side chains with the more hydrophobic amino acids producing silicas with higher surface areas. The more hydrophobic amino acids appeared to reduce inter-particle interaction and condensation resulting in more open framework structures being produced. Increasing the chain length of the homopeptide from 1 to 5 resulted in material with increasingly smaller surface areas but pore volumes which showed no general trend, which is in line with the data reported in the literature.[22] The pore size domains however became more disperse with a trend towards a larger average diameter.

SEM data show an increase in granularity of the materials with the nitrogen containing amino acids suggesting an ability to stabilise aggregates. Silica condensed with L-lysine oligomers also showed this granularity with no change in average granule size observed with increasing chain length. Poly L-lysine however produced spherical porous spheres of up to 1.5 μm which appeared to be made up of smaller aggregates. The aggregation of small aggregates into larger ones could be accomplished by the formation of chains of aggregates connected by entrained poly L-lysine strands. These would tend to form spheres through entropic effects once the charge on the lysine side chains becomes reduced by the presence of silica. The absence of such large scale structures for silicas produced in the presence of L-lysine oligomers shows that merely being able to electrostatically bridge the aggregates is insufficient.

In previous silicification studies using silicon catecholate-complexes as the silica precursor, we have shown that the counter ions of the complex have a profound effect on the kinetics and the final product properties.[28] In particular, the ions (NH_4^+, Et_3NH^+, *etc.*) get associated with the surfaces of silica oligomers/particles by electrostatic attractions and produce silicas with vastly reduced surface area as found in the current study using lysine oligomers. It should be noted that all these precursors, including the one used in this study were water soluble and dissociate to produce orthosilicic acid upon neutralisation, unlike their organosilane counterparts. The presence of cationic species in *in vitro* studies has been found to decrease the rate of dissolution of orthosilicic acid, thus increasing the rate of particle growth.[29] However the mechanism by which this occurs still remains unclear.[8,29]

In addition to understanding the role of biomolecules in silicification, various applications have been developed in the process of learning from biology. These applications include the fabrication of a polymeric hologram with biocatalytically formed ordered silica arrays,[36] C_{60} fullerene–silica hybrid materials,[37] porous silica synthesised using biomimetic surfactants,[23] supports for enzyme[38] and strange shaped silicas produced using peptides.[25,33] We believe that our findings as reported here will be helpful not only in understanding (bio)silicification but also to achieve better sophistication of *in vitro* silica production.

Although, as to the mechanisms for biosilicification, simple chemical[39] and physical[40] models have been proposed in the literature, it is possible that there may be more than one mode of control—with a complex combination of various parameters being possible. It is clear that all amino acid functional groups in proteins that are accessible to silica during the stages of formation from orthosilicic acid through to the final material

Table 3 Summary of effects of amino acids and homopeptides on silica condensation

Additive	3rd order rate constant	Aggregation rate	Surface area	% organic residue
Blank	—	—	—	~
Gly	↓	↔	↑	~
Ala	↓	↔	ND	~
Thr	↓	↔	↑	~
Tyr	↑	↔	ND	22%
Pro	↔	↔	↑	~
Ser	↔	↔	↓	~
Arg	↑	↑	↓	~
Gln	↑	↔	↓	~
Asn	↑	↔	ND	~
Lys	↑	↑	↓	~
Glu	↓	↔	↓	~
$(Gly)_2$	↓ But increase in glycine oligomer	↔	ND	~
$(Gly)_3$	number showed no effect.	↔		~
$(Gly)_4$		↔		~
$(Gly)_5$		↔		0.5%
$(Lys)_2$	↑ Increases with lysine oligomer	Increases with lysine	Decrease with increasing	~
$(Lys)_3$	number	oligomer number	oligomer number	Increasing with lysine
$(Lys)_4$				oligomer number
$(Lys)_5$				
$(Lys)_{poly}$	↓ Due to complex precipitation	Affected by precipitation	Affected by precipitation	

[a] ND Not determined. ↑ Increased, ↓ decreased, ↔ unaffected, ~ negligible.

have a role to play in determining the physical nature and structure of the material that forms. We believe that in biosilicification, amino acids may have a similar role to play *in vivo*. The combination of their effects in (bio)silicification and their intra- and inter-molecular 'arrangements' *in vivo* may be key features to controlling biosilicification.

Conclusions

The purpose of this study was to understand the role of biomolecules in biosilicification *via* individual and oligomeric amino acid effects on *in vitro* silicification. The main findings are presented in Table 3.

Individual amino acids variously reduced or accelerated the early kinetics of condensation and aggregation and produced silicas with surface areas which varied according to the isoelectric point of the amino acid. Introduction of $(lys)_n$ produced a slightly increased enhancement of the early kinetics but dramatically increased aggregation rates as silica condensation progressed, suggesting that aggregation may be a major influence on biosilica formation. Surface areas of the silicas were affected by the amino acids according to their hydrophobicities and a degree of control over both suface area, average pore size and size dispersity were exerted by the addition of lysine homopeptides of varying lengths. Effects on the morphologies of the silicas was observed even with individual amino acids, and with nitrogen containing amino acids producing granular materials.

Acknowledgements

The authors would like to thank Ineos Chemicals, the American Air Force and the European Union for funding of this project.

References

1 H. A. Lowenstam and S. Weiner, *On biomineralization*, Oxford University Press, New York, 1989.
2 P. Calvert and S. Mann, *J. Mater. Sci.*, 1988, **23**, 3801.
3 C. C. Perry, D. Belton and K. Shafran, in *Silicon Biomineralization*, ed. W. E. G. Müller, Springer Verlag, New York, 2003.
4 J. C. Weaver and D. E. Morse, in *Silicon Biomineralization*, ed. W. E. G. Müller, Springer Verlag, New York, 2003.
5 *Silicon and Siliceous Structures in Biological Systems*, ed. T. L. Simpson and B. E. Volcani, Springer-Verlag, New York, 1981.
6 F. E. Round, R. M. Crawford and D. G. Mann, in *The Diatoms: Biology & Morphology of the Genera*, Cambridge University Press, New York, 2003.
7 F. E. Round, R. M. Crawford and D. G. Mann, in *The Diatoms: Biology & Morphology of the Genera*, Cambridge University Press, New York, 1990.
8 C. C. Perry and T. Keeling-Tucker, *J. Biol. Inorg. Chem.*, 2000, **5**, 537.
9 C. C. Perry, J. Moss and R. J. P. Williams, *Proc. R. Soc. London*, 1990, **B241**, 47.
10 C. C. Perry, *Rev. Mineral.Geochem.*, 2003, **54**, 291.
11 T. Kendall, *Industrial Minerals*, March 2000, pp. 49.
12 C. C. Harrison (now Perry), *Phytochemistry*, 1996, **41**, 37.
13 C. C. Perry and T. Keeling-Tucker, *Colloid Polym. Sci.*, 2003, **281**, 652.
14 K. Shimizu, J. Cha, G. D. Stucky and D. E. Morse, *Proc. Natl. Acad. Sci. USA*, 1998, **95**, 6234.
15 R. E. Hecky, K. Mopper, P. Kilham and E. T. Degens, *Marine Biol.*, 1973, **19**, 323.
16 D. M. Swift and A. P. Wheeler, *J. Phycol.*, 1992, **28**, 202.
17 N. Kroger, S. Lorenz, E. Brunner and M. Sumper, *Science*, 2002, **298**, 584.
18 C. C. Perry and T. Keeling-Tucker, *Chem. Commun.*, 1998, 2587.
19 N. Poulsen, M. Sumper and N. Kroger, *Proc. Natl. Acad. Sci. USA*, 2003, **100**, 12075.
20 J. N. Cha, K. Shimizu, Y. Zhou, S. C. Christiansen, B. F. Chmelka, G. D. Stucky and D. E. Morse, *Proc. Natl. Acad. Sci. USA*, 1999, **96**, 361.
21 L. Sudheendra and A. R. Raju, *Mater. Res. Bull.*, 2002, **37**, 151.
22 T. Coradin, O. Durupthy and J. Livage, *Langmuir*, 2002, **18**, 2331.
23 T. Coradin, C. Roux and J. Livage, *J. Mater. Chem.*, 2002, **12**, 1242.
24 S. V. Patwardhan and S. J. Clarson, *Silicon Chem.*, 2002, **1**(3), 207.
25 J. N. Cha, G. D. Stucky, D. E. Morse and T. J. Deming, *Nature*, 2000, **403**, 289.
26 T. Coradin and J. Livage, *Colloids Surf. B*, 2001, **21**, 329.
27 T. Mizutani, H. Nagose, N. Fujiwara and H. Ogoshi, *Bull. Chem. Soc. Jpn.*, 1998, **71**, 2017.
28 C. C. Harrison (now Perry) and N. Loton, *J. Chem. Soc., Faraday Trans.*, 1995, **91**, 4287.
29 R. K. Iler, *The Chemistry of Silica*, John Wiley & Sons, New York, 1979.
30 S. Brunauer, P. H. Emmett and E. Teller, *J. Am. Chem. Soc.*, 1938, **60**, 309.
31 E. P. Barrett, L. G. Joyner and P. P. Halenda, *J. Am. Chem. Soc.*, 1951, **73**, 373.
32 J. Kyte. and R. Doolite, *J. Mol. Biol.*, 1982, **157**, 105.
33 (*a*) S. V. Patwardhan, N. Mukherjee, M. Steinitz-Kannan and S. J. Clarson, *Chem. Commun.*, 2003, 1122; (*b*) S. V. Patwardhan and S. J. Clarson, *J. Inorg. Organomet. Polym.*, 2002, **12**, 109.
34 S. V. Patwardhan, C. Raab, N. Hüsing and S. J. Clarson, *Silicon Chem.*, in press; S. V. Patwardhan and S. J. Clarson, unpublished data.
35 M. Sumper, S. Lorenz and E. Brunner, *Angew. Chem., Int. Ed.*, 2003, **42**, 5192.
36 L. L. Brott, D. J. Pikas, R. R. Naik, S. M. Kirkpatrick, D. W. Tomlin, P. W. Whitlock, S. J. Clarson and M. O. Stone, *Nature*, 2001, **413**, 291.
37 S. V. Patwardhan, N. Mukherjee, M. F. Durstock, L. Y. Chiang and S. J. Clarson, *J. Inorg. Organomet. Polym.*, 2002, **12**, 49.
38 H. R. Luckarift, J. C. Spain, R. R. Naik and M. O. Stone, *Nature Biotechnol.*, 2004, **22**, 211.
39 M. Sumper, *Science*, 2002, **295**, 2430.
40 R. Gordon and R. W. Drum, *Int. Rev. Cytol.*, 1994, **150**, 243.